Fuel 322 (2022) 124169

Contents lists available at ScienceDirect

Fuel

journal homepage: www.elsevier.com/locate/fuel

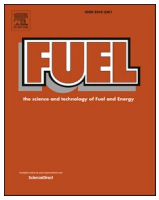

Full Length Article

The combustion of waste, industrial glycerol in a fluidised bed

T. McCann [a,1], E.J. Marek [a,*], Yaoyao Zheng [b], J.F. Davidson [a,2], A.N. Hayhurst [a]

[a] Department of Chemical Engineering and Biotechnology, University of Cambridge, Philippa Fawcett Drive, Cambridge CB3 0AS, UK
[b] Department of Engineering, University of Cambridge, Trumpington Street, Cambridge CB2 1PZ, UK

ARTICLE INFO

Keywords:
Fluidized bed
Agglomeration
Combustion of a liquid waste
Glycerol
Defluidization

ABSTRACT

Large quantities of glycerol are produced as a somewhat useless, industrial by-product, when producing biodiesel. Thus, the combustion of this waste (containing glycerol, less volatile, non-glyceride oils, ash and water) in a fluidised bed has been investigated. The fuel entered the bottom of the bed (on its axis) as bubbles of vapour, which rose up the bed, surrounded by bubbles of fluidising air. While more difficult to burn than medicinal glycerol, continuous burning of the waste was sustained for a total of ~ 4 h in a bed of silica sand (500 – 710 μm) at 750°C, fluidised by air. However, after ~ 4 h, fluidisation ceased, because the silica sand agglomerated into globules a few mm wide, probably cemented by a eutectic of K_2SO_4 and KOH; this industrial glycerol did originally contain potassium and sulphate ions, from its manufacture. Under similar conditions, when burning the waste in a bed of fluidised alumina (Al_2O_3) particles (355 – 425 μm), the bed de-fluidised after almost ½ h, and then sintered into a cake, again possibly cemented by the potassium salts K_2SO_4 and KOH. As for combustion, there was evidence that waste glycerol can be burned in a fluidised bed of SiO_2 particles autonomously, without supplying heat. In such a fluidised bed, it appeared that glycerol vapour, inside a bubble, first decomposes thermally, yielding CO and H_2. The less volatile oils were slower to evaporate and decompose. Combustion of the waste fuel with air occurred in a bed of SiO_2 particles only to a limited extent in rising bubbles, depending on the bed's depth. Otherwise, burning occurred above the fluidised particles, just as a mixture of methane or propane in air burns, when fluidising a hot bed of silica particles. The role of the particles is to inhibit combustion by scavenging radicals.

1. 1.Introduction

Fluidised beds are appropriate for burning solid fuels, because the bed transfers heat to immersed cooling tubes so efficiently that a large rate of heat generation can be accommodated in a small volume [1]. One somewhat unexplored aspect of fluidised beds is the burning of liquid fuels, particularly wastes, in them. This work concentrates on glycerol (CH_2OH-$CHOH$-CH_2OH), which is a waste by-product from the *trans*-esterification of biomass, employed industrially for producing biodiesel. This waste glycerol comprises up to 10 wt% of the *trans*-esterification products [2]. Recently, the production of biodiesel has increased rapidly, because of its appeal as a source of renewable energy [3,4], but the demand for glycerol has not grown in step [2,5]. In 2011, 1.5 Mte of glycerol were produced [2], yet, the potential use for impure glycerol is limited [5], so it is commonly transformed into methane and hydrogen *via* anaerobic digestion [5,6]. This is a promising process, but is apparently not yet feasible on a large scale [6].

An alternative way of extracting energy from waste glycerol is burning it in a fluidised bed. Fluidised beds are appropriate for burning wastes, because their large heat capacity stabilises combustion, particularly when the fuel's properties vary [7]. A fluidised bed might be especially useful with a viscous fuel, such as glycerol, because atomising it is problematical. The use of a fluidised bed can also facilitate the control of pollutants, if the operating conditions are selected carefully [7].

This study follows that of Gibson *et al.* [8], who first burned medicinally pure glycerol in a fluidised bed. They injected a thin jet of liquid glycerol from a nozzle protruding into the bottom of an electrically heated bed of alumina particles (Al_2O_3, 355 – 425 μm) fluidised by air. This achieved stable combustion and, in fact, temperatures for the bed were explored at up to 900 °C. However, problems arose from the glycerol entering the bed as fairly large bubbles of vapour, which were slow to mix with the fluidising air, which also existed mainly as bubbles

* Corresponding author.
E-mail address: ejm94@cam.ac.uk (E.J. Marek).
[1] Present address: AFRY Solutions UK Ltd, 4th floor, West Point, Springfield Road, Horsham RH12 2PD.
[2] In memoriam; obiit, 25 December 2019.

https://doi.org/10.1016/j.fuel.2022.124169
Received 26 October 2021; Received in revised form 16 March 2022; Accepted 7 April 2022
Available online 14 April 2022

Nomenclature

C	concentration of volatile species, mol m^{-3}
D	diffusion coefficient, m^2 s^{-1}
d	diameter of a bubble in a fluidised bed, m
d_c	diameter of the cloud around a fast bubble, m
G	volumetric flowrate of vapour into a bed, m^3 s^{-1}
g	acceleration due to gravity, 9.806 m s^{-2}
k	mass transfer coefficient, m s^{-1}
Sh	Sherwood number $= k\ d_c/D$
t	time, s
U	superficial velocity of fluidising air through a hot bed, m s^{-1}
U_b	rise velocity of a bubble, m s^{-1}
U_{mf}	value of U for incipient fluidisation, m s^{-1}
V_b	volume of a bubble after being first formed, m^3
ε	voidage in the particulate phase of a fluidised bed
θ	equivalence ratio $=\frac{\text{Actual ratio of (fuel/air) in the feed to the bed}}{\text{Ratio of (fuel/air) for stoichiometric combustion}}$

[8]. The result was that glycerol often burned undesirably at the top of the bed or well above it. Interestingly Gibson *et al.* [8] deduced that in the rising bubbles of pure glycerol, its vapour decomposed thermally to give mostly CO and H_2. Some of the H_2 appeared to diffuse in between the particles of fluidised alumina, where it burned, *i.e.* in the particulate phase, but the less diffusive CO did not [8]. This is because free radicals recombine on the fluidised particles, thereby inhibiting the combustion of CO [9]. Thus, CO only burns in bubbles containing some air [9] or above the bed in the freeboard. When burning medicinal glycerol in a bed at 700 – 900 °C, little CO was detected far downstream of the bed [8], provided there was>43% excess air, so that all the CO was then oxidised to CO_2, but this occurred partly in the freeboard. However, with less than 43% excess air, CO was detected in the gases on leaving the bed, i.e. some CO was produced inside the bed. Gibson *et al.* [8] found the optimal temperatures for combustion within the fluidised bed were above 850 °C for fuel-rich conditions, and any temperature in the range 700–900 °C for fuel-lean combustion.

As for previous work, Bohon *et al.* [10] also achieved stable combustion of glycerol, but in a high-swirl burner with a refractory-lined furnace. They found difficulties with auto-ignition and with glycerol's high viscosity [10]. Menon *et al.* [11] attempted batch-wise combustion of glycerol in an electrically-heated fluidised bed of alumina sand, and found mixing problems below 800 °C, again because of glycerol forming large bubbles of vapour, whose contents did not readily mingle with the fluidising air. Above 800 °C, the glycerol was observed burning in small bubbles below the top of the fluidised bed [11]. These mixing problems were also found by Stubington and Davidson [12], when burning kerosene in a fluidised bed of sand at 940 °C. Of course, such mixing problems can be mitigated for continuous combustion by carefully designing the injection nozzle [13,14]. A potential problem is that glycerol can burn and yield acrolein [15], which is toxic and an irritant [16]. However, its characteristic harsh smell was not detected by Gibson *et al.* [8], who concluded that acrolein burns rapidly away in a bed fluidised by air, when above 600 °C. It should be mentioned that Żukowski and Berkowitz [17] have recently burned pure glycerol in a fluidised bed of cenospheres. These are hollow spheres of an aluminosilicate, formed from coal waste; their size was 0.25 – 0.30 mm and density below 900 kg/m^3. Some cenospheres were coated with "a catalytic layer of iron oxide". Pure glycerol burned in fluidised beds of either coated or uncoated cenospheres, but the burning of waste glycerol in either type of bed was not reported [17].

The most common problems, when burning liquid fuels in fluidised beds, are blocking of the feeding nozzle and agglomeration of the fluidised particles [13]. These issues are worse with more viscous fuels. This study encountered two such problems: (1) blockage of the nozzle feeding the industrial glycerol, (2) sintering of the fluidised particles during prolonged (4 h) operation. Sintering has been observed often when burning coal or biomass [18–20]; also alumina and silica sands can agglomerate above 800 °C, when burning straw [21,22].

2. Experimental

2.1. Characterisation of glycerol

Medicinal glycerol (Stada Arzneimittel AG) was used for starting up the combustion of waste glycerol in a fluidised bed. Industrial glycerol was supplied by Argent Energy Ltd, Motherwell, Scotland. It had been retrieved at the end of a run producing biodiesel. As delivered, it was dark brown, opaque and had a strong smell, whereas medicinal glycerol is colourless, clear and odourless. The waste glycerol contained fine solids, which were filtered out. According to its producer, the waste glycerol contained 58 wt% glycerol, 21 wt% water, 14 wt% miscellaneous, organic non-glycerides (waste oils), and the remaining 7 wt% as ash (largely potassium sulphate). The *p*H of the glycerol as received was measured to be 5.2; the approximate boiling point of industrial glycerol was determined to be ~ 190 °C [23], *i.e.*, significantly lower than for pure glycerol (290 °C).

Thermogravimetric analysis (TGA) of both glycerols was performed with a Mettler Toledo TG analyser (DSC1) with a horizontal reaction chamber. Thus, a sample of ~ 50 mg was placed in an alumina crucible and heated at a constant rate of 10 °C min^{-1} from 50 to 800 °C. The analyser was continuously purged with Ar (100 mL min^{-1} at NTP) and during the experiment a carrier gas, N_2 (50 mL min^{-1} at NTP) was passed over the sample to avoid combustion. The measurements of the sample's mass in Fig. 1 reveal that the medicinal glycerol was completely vaporised by 300 °C. However, a white and brittle solid residue was left (at up to ~ 800 °C) by the industrial glycerol, amounting to ~ 8 wt% of the original mass. Also visible from Fig. 1 with waste glycerol is an initial mass loss below 120 °C, representing the evaporation of water. This is consistent with the sample containing 21 wt% water. Otherwise, glycerol appears to evaporate from the waste above ~ 200 °C, and the process is completed on reaching ~ 320 °C.

To analyse the solid residue left after evaporating waste glycerol, a sample of the solid was obtained from the TGA, but using air as the carrier gas, when heating from 50 °C to 850 °C at a rate of 20 °C min^{-1}, and then leaving it at 850 °C for 2 h. At the end, the residue's mass was constant at 5 wt% of the initial mass, close to the declared ash content of 7 wt%. The solid residue (~2 mg) was dissolved in 2 mL of 70 wt% nitric acid and diluted with 50 mL Milli-Q water. The solution was further diluted tenfold using 1 M HNO_3. The result was analysed using an ICP-MS (inductively coupled plasma mass spectrometer) (Perkin Elmer Nexion 350D), in a "TotalQuant" mode, with a quadrupole mass spectrometer, giving, a Semi-Quantitative full mass spectral scan. This instrument is good at detecting metals; its limits of detection for most metallic chemical elements were better than 1 part per trillion. The main components of the residue were found to be: 8.8 wt% K, 0.4 wt% Ca, 0.2 wt% Na, and 0.1 wt% for each of P and Al. The high value for potassium derives from potassium hydroxide having been used as the catalyst for the *trans*-esterification step producing biodiesel. The rest of the residue is probably an element (not as readily detected by ICP-MS as is a metal) such as: (i) oxygen, with the white residue powder being oxides of the detected elements, and (ii) sulphur (as sulphate ions, containing much oxygen). According to the waste's manufacturer, sulphur typically accounts for 2–4 wt% of waste glycerol. The sulphate ions probably derive from sulphuric acid having been used in the production of biodiesel.

2.2. The fluidised bed

The bed has been described before [8,23], but is illustrated in Fig. 2. The fluidised particles were contained in a stainless steel tube (i.d. 78

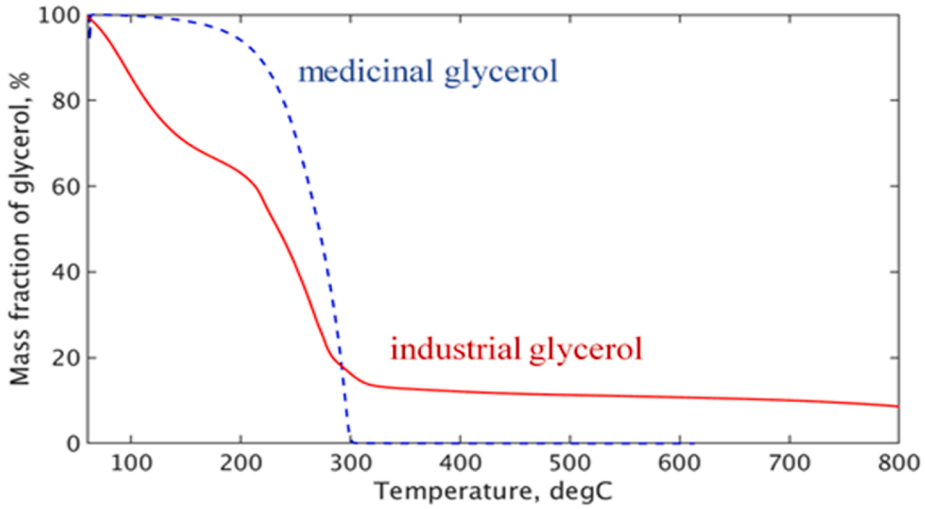

Fig. 1. Relative masses of industrial and medicinal glycerol during heating at 10 °C min^{-1} in N_2, as measured in a TGA.

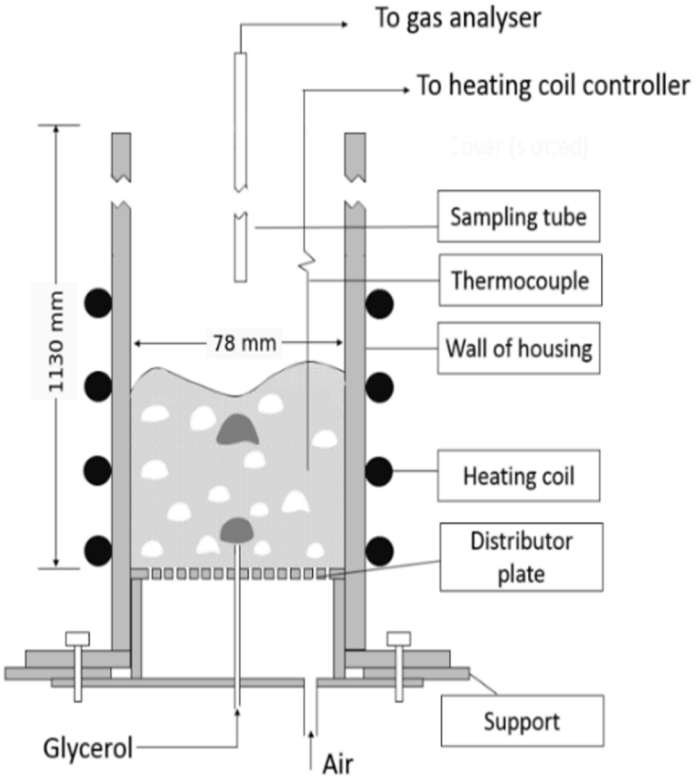

Fig. 2. Sketch of the fluidised bed and the pipe feeding glycerol to just above the distributor. Bubbles of glycerol vapour in the bed are shown dark. They rise up the middle of the bed and are surrounded by bubbles of air (white). Air also percolates between the fluidised particles to fluidise them, normally at a temperature of 750 °C.

mm), heated with external, electric coils. The heating was controlled with a Neutronic 96 PID controller, coupled with a K-type thermocouple, immersed in the bed of particles. Two types of solid were fluidised: alumina sand (Boud Minerals, density of a particle 3980 kg m^{-3}, sieved to 355 – 425 μm) and silica sand (from King's Lynn, UK; particle density 2400 kg m^{-3}, selected size 500 – 710 μm). Typically, 1 L of particles were in the bed, resting on a stainless steel distributor plate with a square-pitch array of 36 holes of diameter 0.4 mm. All experiments were performed at 750 °C. Glycerol was introduced into the bed through a stainless steel, feed-pipe (o.d. 3.18 mm, i.d. 1.59 mm), mounted in the centre of the distributor plate. It was possible to reduce the feeder's i.d. by inserting different "nozzles" into its tip. The minimum velocity for incipient fluidisation of SiO_2 particles at 750 °C was found to be $U_{mf} = 0.13$ m s^{-1}; for Al_2O_3 particles, $U_{mf} = 0.11$ m s^{-1}. Both these values were measured (correct to 10%), using the pressure difference between the bottom of the fluidised bed (using the empty feed-pipe as a pressure tapping) and atmospheric pressure [23], when the velocity of the fluidising air was decreased in steps. Usually, $U/U_{mf} = 2.7$ in the experiments described below; this meant that the depth of the bed was ≈25 cm, when fluidised, but ≈ 20 mm when not fluidised. For a bed of Al_2O_3 particles, U/U_{mf}, was 2.5, similar to a bed of silica particles. Every bed was fluidised using the laboratory's compressed air supply.

That a bed was a bubbling one was checked regularly.

Glycerol was drawn from a beaker using a Watson-Marlow 101U peristaltic pump. In contrast to previous work [8], the feed-pipe protruded into the bed ~ 10 mm above the distributor. Also, the tip of the feeder was consequently hotter. The flowrate of glycerol was often varied, whilst keeping that of the air constant at 0.0217 mol s^{-1}; this enabled the overall stoichiometry for combustion to be varied. Here the fuel-richness was defined by the equivalence ratio as:

$$\frac{\text{Actual ratio of (fuel/air) in the feed to the bed}}{\text{Ratio of (fuel/air) for stoichiometric combustion}} = \frac{\text{Fuel supplied}}{\text{Fuel for a stoichiometric mix with O2 supplied}} \quad (1)$$

A list of conditions investigated in the combustion experiments is provided in Table 1.

Heat-transfer calculations [23] indicated that the highest rate of feeding waste glycerol (0.146 g s^{-1}) resulted in the fuel entering the bed at ≈ 75 °C, *i.e.*, as liquid, which rapidly evaporated in a bed at 750 °C. The formula of Davidson and Harrison [24] gives the volume of a gaseous bubble (in m^3) on detaching from an orifice to be:

$$V_b = 0.289 G^{6/5} \quad (2)$$

Here G (m^3 s^{-1}) is the volumetric flowrate of vapour flowing into the bed. Equation (2) indicates that the bubbles of vapour, initially formed at the bottom of a bed, have a diameter of up to 25 mm for the highest flow rate of glycerol, *i.e.* for the most fuel-rich situation. In general, a stream of bubbles of vapour from industrial glycerol rose up the middle of the bed; they were surrounded by bubbles of air, as shown in Fig. 2. According to Eq. (2), the bubbles of air were formed at the orifices in the distributor with an initial diameter of ~ 15 mm.

2.3. Mixing of gases in a fluidised bed

The rise-velocity of a bubble of diameter, d, is [24]:

$$U_b = 0.71\ (gd)^{1/2} \quad (3)$$

This means that with *e.g.* $d = 15$ mm, a newly formed bubble of air rises up the bed with a velocity $U_b = 0.27$ m s^{-1}. This gives $(\varepsilon U_b / U_{mf}) \sim 0.86$, so U_b is slightly slower than the ratio $(U_{mf} / \varepsilon) \sim 0.32$ m s^{-1}, where ε is the voidage in the particulate phase and was taken as 0.41 ± 0.01 [24,25]; also $U_{mf} \sim 0.13$ m s^{-1} for particles of SiO_2 being fluidised, but $U_{mf} \sim 0.11$ m s^{-1} for Al_2O_3. The ratio (U_{mf} / ε) is the mean velocity of the fluidising air flowing through the particulate phase, *i.e.* between the particles in a bed. Because here $U_b < (U_{mf} / \varepsilon)$, the air bubble is said [24,25] to be "slow" or "small". Broadly speaking, the faster moving gas from the particulate phase then moves quickly upwards and straight through such a void, directing most of its contents into the gaps between the surrounding fluidised particles [24,25]. However, this small bubble does contain a little torus of gas, which actually remains inside the bubble. In fact, within this toroidal ring there is merely internal circulation of gas [24,25]. On the other hand, a large bubble, *i.e.* with $(\varepsilon U_b / U_{mf}) > 1$, is not exactly spherical; it is actually the shape of a kidney. It is always surrounded by a "cloud" of fluidised particles [24,25], with a thickness, which decreases as $(\varepsilon U_b / U_{mf})$ increases. Whilst such a fast bubble ascends up a bed, together with its "attached" cloud, gas circulates in a toroidal pattern around both the bubble and its cloud, without entering the rest of the bed. This means that the contents of a fast bubble and its cloud do not readily mix with the bulk of the gas in the particulate phase, although this does happen slightly by molecular diffusion (especially for H_2) and also by the rather severe disturbance when two bubbles collide [24,25].

Table 1
Matrix of experimental conditions used in the combustion experiments.

Bed material	Equivalence ratio, θ	Temperature (°C)	U/U_{mf}
Al_2O_3	1	750	2.5
SiO_2	0–1.2	750	1.3, 2.5–2.7

With a bed at 750 °C, as seen above, the air bubbles are initially small, when first formed, because $(\varepsilon U_b / U_{mf}) = 0.86$. With the usual value of $(U / U_{mf}) = 2.7$, the many bubbles of air soon collide, coalesce and grow, and so soon become large and fast. Consequently, bubbles of air thereafter exchange their contents only slowly with the gas permeating interstitially through the particulate phase between the particles. This exchange is more rapid for smaller, slow bubbles than larger ones [24,25].

The glycerol, either waste or pure, entered a bed as a train of bubbles containing the vapour of the fuel; these bubbles had initial diameters ranging up to ~ 25 mm, when θ was increased to 1.2. Assuming $d = 20$ mm, with $U_b \sim 0.314$ m s^{-1}, gives $(\varepsilon U_b / U_{mf}) \sim$ unity. In such a bubble there is a slightly larger torus than in a void with a diameter of 15 mm. Of course, bubbles coalesce and grow to become "fast", with the result that the mixing of glycerol vapour with interstitial air soon become restricted, once $(\varepsilon U_b / U_{mf})$ becomes unity. Bubbles of air also coalesce and accordingly mix their contents with gas in the particulate phase, until $(\varepsilon U_b / U_{mf})$ for the air bubbles reaches unity. Higher up a bed, a lack of mixing of fuel and oxygen delays combustion; this is additionally inhibited by the solid particles, which remove free radicals by providing a large surface area, where free radicals readily recombine [26]. Finally, it is worth noting that, because U_{mf} is smaller for the particles of Al_2O_3 than of SiO_2, a bubble tends to have a slightly larger value of $(\varepsilon U_b / U_{mf})$ in a bed of these particular Al_2O_3 particles.

The slowness with which the contents of a fast bubble of fuel and its cloud mix with the gas fluidising the particles can be seen from assuming the cloud has diameter d_c ($d_c > d$). Suppose the gas in the spherical bubble and its cloud is well-mixed and contains a diffusive hydrocarbon compound with a concentration, C. Mass transfer from the bubble and cloud of fuel to the particulate phase can be approximated by:

$$-\frac{\pi d_c^3}{6}\frac{dC}{dt} = k\pi d_c^2 C \quad (4)$$

where k is the mass transfer coefficient and C is taken to be zero between the fluidised particles. Equation (4) indicates that mass transfer occurs with a time constant $\tau = (d_c/6k) = (d_c^2/6D \times \text{Sh})$. Here $\text{Sh} = kd_c/D$ is the Sherwood number and D is the diffusivity of the transferred hydrocarbon component. Taking $d_c \sim 25$ mm, Sh to be slightly above 2, say 4, and D for a hydrocarbon to be $\sim 5 \times 10^{-6}$ m^2 s^{-1}, yields $\tau \approx 5$ s. The time-scale is set by the residence time of a bubble of fuel ($U_b \sim 0.314$ m s^{-1}) in the fluidised bed (depth ~ 0.25 m) equal to ≈ 0.25/0.314 ≈ 0.8 s, at the very most. This confirms that the hydrocarbons from a droplet of fuel vapour hardly mix with the fluidising air within the bed, after $(\varepsilon U_b / U_{mf})$ has reached unity.

2.4. Experimental procedures

To start an experiment, first medicinal glycerol was injected into a hot bed and after a few minutes of stable combustion, the fuel was switched to waste glycerol. Such a procedure avoided the feed-tube

being blocked by solid residue from over-heating waste glycerol. The off-gas from a bed was sampled at 1 L min^{-1}, with a movable sampling probe (stainless steel) typically situated ~ 30 cm above the top of the bed. The sampling line included a particle trap and drying unit with anhydrous $CaCl_2$. The off-gas was sent to an ABB gas analyser (EL-3020), to measure the concentrations of CO, CO_2, and O_2 in dried samples taken vertically along the freeboard's centre-line. When combustion had stabilised, the gas composition was measured for 10 min. The equivalence ratio for combustion was changed by varying the flowrate of glycerol, while keeping the flowrate of air constant. During the combustion of waste glycerol, a yellow flame, indicating the presence of soot, was usually visible above the bed, particularly when using high flow rates of glycerol. That a flame sat on top of a bed indicated that much of the fuel was burning above the bed, rather than within it. As discussed below, quite loud "popping" sounds were also heard to accompany mini-explosions in the gas leaving the fluidised particles. These brief "pops" indicated that hydrogen was then actually burning in oxygen.

2.5. Characterisation of a bed's particles after combustion experiments

After being fluidised and combustion occurring, particles of SiO_2 and Al_2O_3 were analysed using scanning electron microscopy (SEM). The images were acquired with a Leo GEMINI 1530 VP at an accelerating voltage of 4.0 kV and a working distance of 5.0–8.0 mm. Samples were mounted on copper tape for Energy-dispersive X-ray spectroscopy (EDS), for which the acquisition and analysis of spectra were performed using an Oxford Instruments Aztec (Energy X–maxN).

Phase identification of particles in a sinter after burning waste glycerol in them was done on X-ray powder diffraction (XRD) patterns. Scans were collected with a PANalytical Empyrean diffractometer, using Cu-Kα radiation with a voltage of 40 kV and current 40 mA. Phase identification was performed with Topas Academic V5 software. Rietveld or Pawley refinement was performed using reference structures from the ICSD database, *i.e.* Al_2O_3 (ICSD 10425), KOH (ICSD 61047), K_2SO_4 (ICSD 2827), SiO_2 (ICSD 116331). Accounting for other components did not improve the quality of fit. For example, EDS results indicated that agglomerated SiO_2 particles retrieved from a bed after burning glycerol were partially covered by a component containing K, S and O. However, the best fit in the Rietveld refinement for the same sample was obtained for SiO_2 only, indicating that the layer of the salt containing K plus S (most likely K_2SO_4), detected with EDS, was thin, most likely less than 0.05 μm, so the approximate penetration depth of the applied electron beam.

3. Results and discussion

3.1. Combustion in beds of Al_2O_3 particles

With alumina particles in the bed, it was found that the combustion of industrial glycerol could not be sustained for longer than 30 min, when the particles agglomerated. After this, the cake of particles impeded the flow of glycerol through its inlet into the bed, resulting in glycerol pyrolysing inside its feeding-tube and depositing solids there. After the bed had cooled, it was found that a solid layer of agglomerated particles (depth 1–2 cm) covered the distributor plate. Parts of an alumina cake are shown in Fig. 3, which is very similar to photographs of agglomerates [27,28] from the quite different combustion of solid fuels, such as biomass or a low-rank coal. The blackish agglomerate in Fig. 3 was lightweight and brittle; it was easily broken by hand.

An XRD analysis of a cake of Al_2O_3 is shown in Fig. 4a, which establishes the presence of K_2SO_4, KOH and Al_2O_3. However, it is worth noting that potassium aluminate was not detected using XRD; nor were potassium silicate in Fig. 4b (for a sinter from a bed of SiO2 particles) or the oxide, K_2O in Fig. 4a or 4b.

Fig. 5a shows typical results from the EDS surface mapping of a small area of a particle from a cake of Al_2O_3 particles. The location of the element Al is clear. Its spatial distribution correlates positively with that of the element oxygen, indicating the location of an exposed Al_2O_3 surface. Also, the distributions of S and K are similar to each other and correlate negatively with those of Al and O from Al_2O_3. The element oxygen appears almost everywhere. Interestingly, carbon in the form of coke was also present and appears to be evenly distributed; this explains the black colour of the retrieved alumina cakes (as seen in Fig. 3). Observations from Fig. 5a might be explained by the particles in a cake being cemented with K_2SO_4. In addition, KOH could be fulfilling such a role, bearing in mind that KOH and K_2SO_4 are stable at flame temperatures [29] of ~ 2000 K. The compounds have melting points of 1069 °C (K_2SO_4) and 400 °C (KOH, with a boiling point of 1330 °C). Interestingly K_2O decomposes at 350 °C and, because it was not detected in Fig. 4a or 4b, can probably be neglected. Likewise, K_2S need not be considered, from its absence in both parts of Fig. 4. This sulphide might well have resulted from hydrogen reacting with K_2SO_4 in the hot reducing conditions inside a rising bubble of fuel. However, it is quite possible that KOH and K_2SO_4 form a sticky eutectic, with the additional possibility of bonding to the "inert" fluidised particles. Here then is one way whereby sinters might form [28], *viz*. by being cemented together with either K_2SO_4, or KOH plus K_2SO_4. The possibility that K_2SO_4 or KOH might by reacting with Al_2O_3 to provide the cement for agglomeration is unlikely here, given that potassium aluminates were not detected by XRD.

3.2. Combustion in beds of SiO_2 particles

Industrial waste glycerol burned in a bed of SiO_2 particles for as long as 4 h. During that time, no problems from the fluidised particles sintering were encountered, nor were there difficulties feeding the glycerol into the bed. It was observed that the PID temperature controller did not activate the electric heating coils during combustion. It was accordingly concluded that it is definitely possible to burn industrial waste glycerol

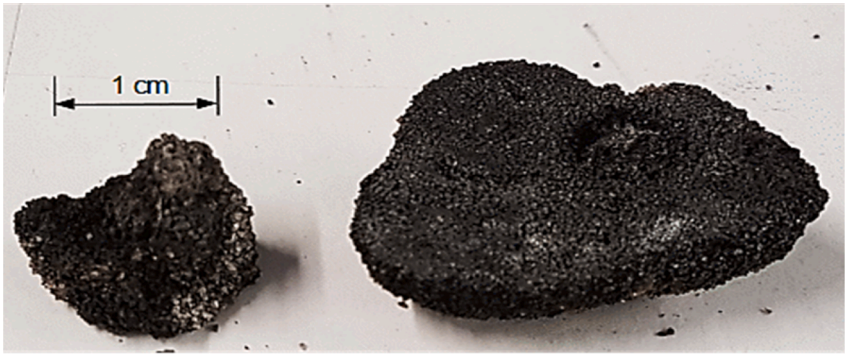

Fig. 3. Agglomerated lumps/cakes of alumina sand extracted from the fluidised bed after burning industrial glycerol for 30 min. The scale for 1 cm is shown to illustrate the size of a lump of sinter.

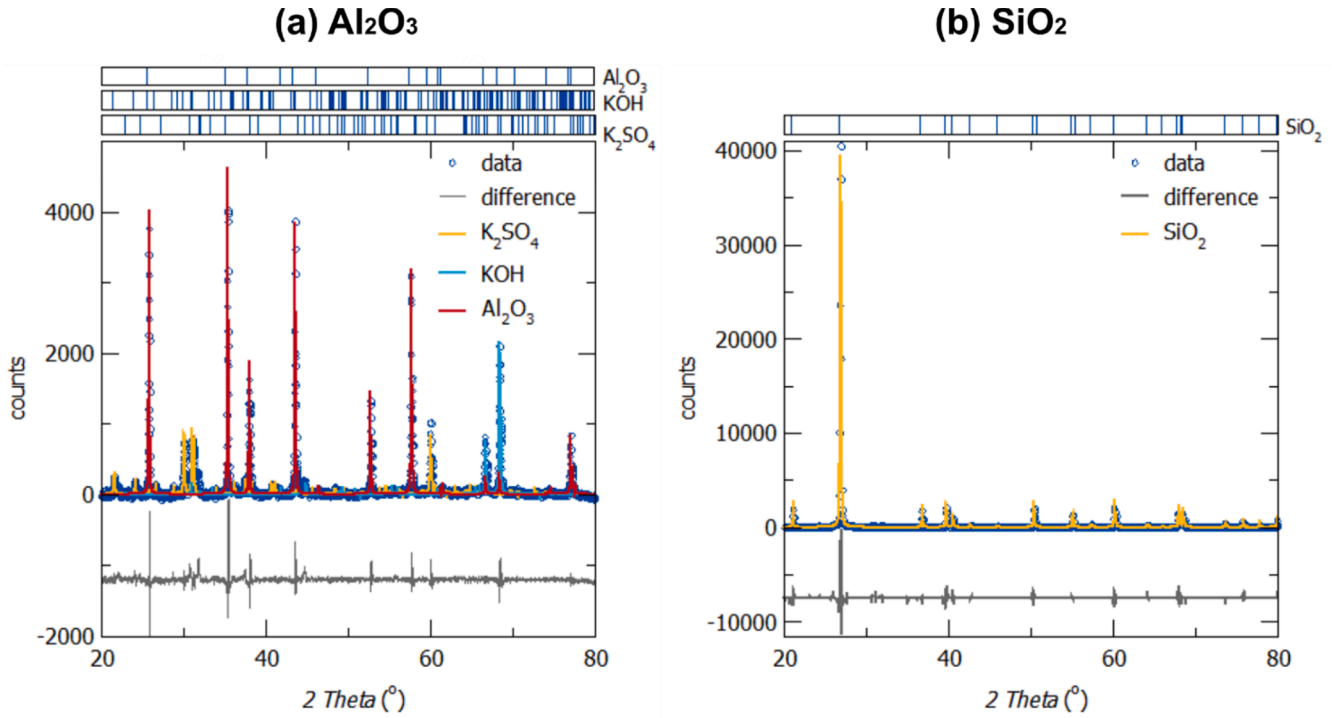

Fig. 4. XRD analyses of the particles in sinters of (a) Al_2O_3, (b) SiO_2.

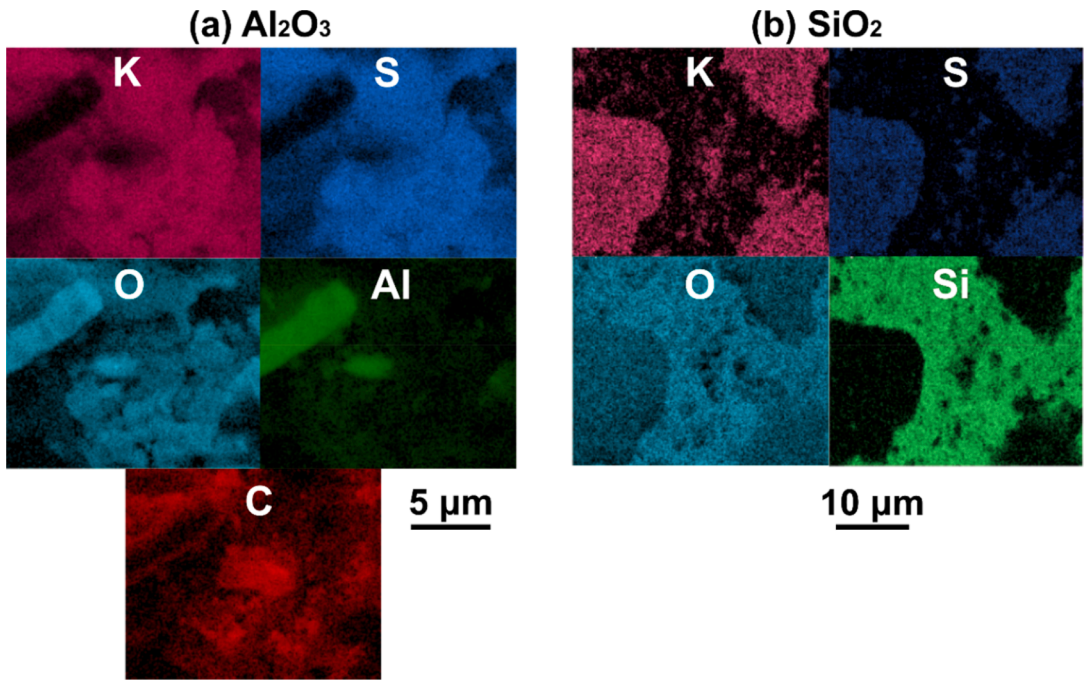

Fig. 5. EDS maps created by scanning the surface of a particle of (a) Al_2O_3, (b) SiO_2 after burning waste glycerol. Each map in Fig. 5a represents ~ 15 × 15 μm^2 of a particle's surface; the area covered by Fig. 5b is 4 times larger. The colours indicate the detected elements, as shown.

inside a fluidised bed in a self-sustainable matter, without any additional heating.

When attempting to use the nozzle inserts in the feed pipe to alter the fuel's flowrate into the bed, the feed pipe blocked as soon as the industrial glycerol reached the nozzle tip. This was observed for nozzles with i.d. 0.3, 0.5, 0.7 and 1.0 mm. This is thought to have been caused by dead zones just before the nozzle, where glycerol heated up and pyrolysed, forming a solid residue, as observed using TGA in Fig. 1. The nozzle inserts were accordingly discarded, so the pipe feeding glycerol was simply a stainless steel tube with i.d. 1.58 mm and o.d. 3.18 mm.

The silica sand eventually changed in appearance, whilst burning waste glycerol, from yellow to light pink/grey, as shown in Fig. 6. Then, the sand became very difficult to fluidise and gas channelling was observed in the bed. Subsequent inspection revealed that the silica sand had agglomerated into small chunks, a few millimetres in diameter. Thus, there is a problem from sand particles agglomerating, but only after a few hours of burning, in contrast to the rapid appearance of cakes of Al_2O_3, seen in Fig. 3. The XRD analysis of the agglomerates, presented

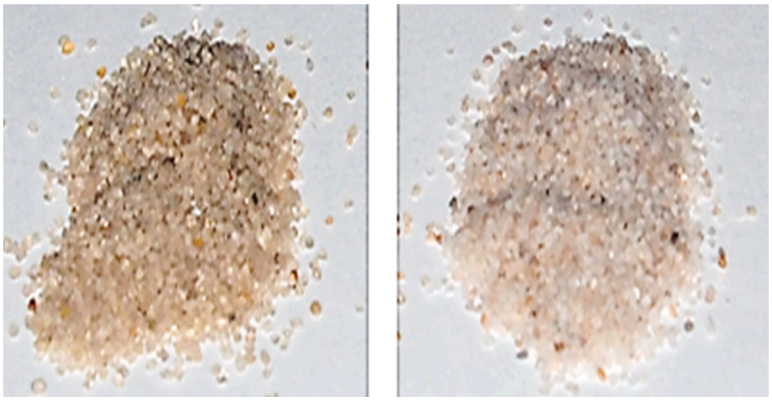

Fig. 6. Silica sand before (left) and after successfully burning industrial glycerol (right).

in Fig. 4b, confirmed the presence of SiO_2 only; no compounds of potassium or sulphur were detected. This indicates that the layer of a new substance bonding together SiO_2 particles was thin, corresponding to a mass content below 3–5 wt%, *i.e.* the detection limit of XRD. The agglomerates were further analysed using microscopic methods, which yielded the EDS maps in Fig. 5b. Just as for a cake of alumina particles, oxygen was ubiquitous. In addition, sulphur and potassium both had similar distributions, which correlated negatively with that of silicon. Even so, Fig. 5b now shows K, S and O overlapping in some areas, rather than being evenly distributed. Coke was not observed, possibly because during the 4 h of a combustion experiment with SiO_2 particles, the bed started channelling, but without the gas flow becoming completely obstructed, in contrast to the situation observed with severely agglomerating Al_2O_3 particles.

That individual particles of SiO_2 survived ~ 4 h could well be a consequence of their size and momentum, with these significantly larger, heavier particles of SiO_2 being harder to stick together (or agglomerate) than smaller ones of Al_2O_3. The cohesive behaviour might possibly be attributed, as suggested previously [22,28], to sticky eutectics formed in:

$$K_2O + nSiO_2 \rightarrow K_2O(SiO_2)_n \quad (5)$$

with n from 1 to 4. The eutectic $K_2O(SiO_2)$ melts at 976 °C [30], but for $K_2O(SiO_2)_4$ the melting point is 764 °C. Thus, these melting points could be low enough to cause the observed sintering. One problem with the suggestion of reaction (5) is that K_2O decomposes at 350 °C. Furthermore, neither silicates nor K_2O were detected in Fig. 4b. However, from Fig. 5b, it does look as if potassium and oxygen, and probably sulphur too, are important in agglomerating particles of SiO_2. Again, this could involve K_2SO_4, and possibly a sticky eutectic with KOH, similarly to the mechanism proposed for cementing Al_2O_3 particles. However, K_2SO_4 alone has been previously found [31] not to bind particles of SiO_2 together, unless potassium reacts with SiO_2 forming a silicate [32], resulting in sintering [30]. However, formation of potassium silicate cannot be the entire explanation of the sintering of silica particles, because waste glycerol did form a solid when overheated in its supply line before reaching the fluidised bed of SiO_2 particles. That alumina forms more tightly bound agglomerates relatively rapidly could result, at least partly, from smaller particles and also weaker bonding between a melt and a surface of SiO_2 than with Al_2O_3.

The colour change (to light, pinkish grey) for yellowish SiO_2 sand has been previously observed after various heat treatments [33]. It seems that traces of iron in the sand might be responding to changes in the sand's temperature [30]. Here the change in colour was associated with particles agglomerating into 3 – 5 mm chunks, and also with the onset of gas-channelling. All the above does indicate a limited lifetime for this size of SiO_2 particles; however, given that sand is actually cheap, replacing it after ~ 4 h is a real possibility.

From our study, no firm conclusion can be made about what is causing the fluidised particles of SiO_2 to agglomerate. It looks as if potassium silicate does not provide an explanation; this leaves a eutectic of KOH and K_2SO_4 as a likely possibility. The other possibility was a eutectic formed in reaction (5). This seems unlikely because of the instability of K_2O. Clearly more work is required.

3.3. Visual observations whilst burning waste glycerol

With a shallow bed (unfluidised depth of particles less than 100 mm) loud "popping" noises were heard, when burning either medicinal or waste glycerol. In addition, yellow (*i.e.* sooty) flames, with hints of blue, were observed above the fluidised particles. It was also possible to see bubbles exploding and accompanying the brief, sharp "popping" sounds, characteristic of hydrogen exploding, but here in bubbles disengaging from a bed at say 750 °C. These explosions have been noted and discussed before [8], together with the blue flashes indicating that CO, as well as hydrogen, was burning in the gases leaving a bed. The explosions were stronger when burning medicinal glycerol and always much less conspicuous above hotter beds and also those in which the sand was deeper. This indicates that H_2, and possibly also CO, burned in bubbles inside a deeper or hotter bed, as opposed to above it. The indications were that low down a bed, bubbles of the "vapours" from glycerol" were heated rapidly to the bed's temperature, but being in a bubble large enough to be a fast one, its contents mixed with the surrounding gas in the particulate phase very slowly [24,25]. In fact, the gas contained in a fast bubble stays there during the bubble's ascent to the top of the bed. However, this gas circulated around the bubble and also the surrounding thin "cloud", where the gas contacted fluidised particles, which acted as scavengers of any free radicals [26]. Even so, thermal decomposition of glycerol in the overall step:

$$C_3H_8O_3 \rightarrow 3\ CO + 4\ H_2 \quad (6)$$

occurred inside a rising bubble. As for the oxidation of very diffusive H_2 or CO or hydrocarbon fragments from the non-glyceride oils, with O_2 from the fluidising air, some mixing did occur when a bubble of fuel vapour collided with one of air. Otherwise, gas in any fast bubble mixes only slowly with that percolating between the fluidised particles. This is why hydrogen only burns within a bed, which is deep and hot. At the top of a more shallow bed, mixing did occur whilst bubbles of every kind disengaged from the fluidised particles. This picture has much in common, with combustion in a bed of hot sand fluidised by *e.g.* a mixture of methane or propane in air [26,34]. Then there is no combustion in the particulate phase between the fluidised particles, because free radicals diffuse to and recombine on any solid surface, thus forming stable molecules. Similarly, combustion in a bubble is suppressed by gas moving towards the particles within the surrounding cloud. However, then combustion can occur if the residence time of gas in the bubble

exceeds the ignition delay time [35]. A significant amount of water enters along with the fuel because the industrial glycerol contains 21 wt % of water. In theory, water might be a source of oxygen for the combustion in the fuel bubbles, because of *e.g.*

$$H + H_2O \rightarrow H_2 + OH \quad (7)$$

providing OH radicals, but only if the temperature reaches ~ 2000 K. However, the rate coefficient of reaction (7) is too small [36] for (7) to be important at 750 °C.

The other visual observation, noted above, was that soot's presence was evident from its characteristic yellow colour (see FigS.1 in the Supplementary Document). Its formation presumably is a consequence of waste glycerol entering the fluidised bed as a succession of bubbles of its vapour, which rise up close to the bed's axis, whilst surrounded by bubbles of air. The fuel consequently pyrolyses, with possibly glycerol producing some hydrogen, which diffuses away and burns, probably between the particles. However, because of the lack of oxygen in a bubble of fuel, the oily component forms soot particles. Also, because some soot is produced, when burning pure glycerol [8], that would have happened here, with waste glycerol as the fuel. In that case glycerol must decompose thermally to produce radicals like CH, CH_2, C_2H, namely, the precursors of soot. Clearly, reaction (6) is not a totally accurate description of glycerol's thermal decomposition. Some of these soot particles evidently persist into a combustion zone immediately above the fluidised sand.

3.4. Sampling the off-gases along the freeboard whilst burning waste glycerol

Fig. 7 shows the concentrations of O_2, CO and CO_2, measured in dried samples taken along the freeboard of the fluidised bed of silica sand, when burning industrial glycerol. In this case, combustion was overall fuel-lean. In fact, for the conditions in Fig. 7, θ was 0.83, calculated assuming that waste glycerol was 100 % pure glycerol. In this case, there was $1/0.83 = 1.20$ times more air than for stoichiometric combustion to CO_2 and H_2O. A mass balance on the element carbon for the complete combustion of medicinal glycerol according to:

$$C_3H_8O_3 + 3.5\ O_2 \rightarrow 3\ CO_2 + 4\ H_2O \quad (8)$$

at $\theta = 0.83$ indicates a total mole fraction for CO and CO_2 (in dried samples) of 0.154. In fact, Gibson *et al.* [8], using this apparatus, measured final mole fractions of 0.160 ± 0.007 for CO_2 and 0.002 ± 0.001 for CO in dried samples leaving the very top of the tube housing

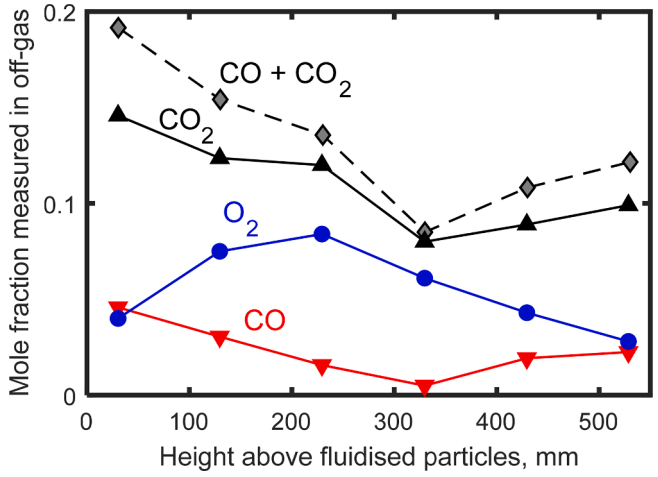

Fig. 7. Mole fractions of O_2, CO and the sum (CO + CO_2), as measured at different heights along the axis above a bed of silica sand (fluidised depth ~ 25 cm) at 750 °C with $\theta = 0.83$ and $U/U_{mf} = 1.3$, when burning industrial glycerol. Averaged values from 10 min measurements with ±0.005 error.

the fluidised bed. Such good agreement indicates the combustion of medicinal glycerol was indeed complete, without any significant production of soot, acrolein or other intermediates. Also, there was no significant participation of H_2O as an oxidiser of glycerol, started by *e.g.* reaction (7) generating OH radicals.

When burning waste glycerol, which contains 58 wt% glycerol, 14 wt % organic, non-glyceride oils of unknown composition, 21 wt% water and 7 wt% ash, in order to calculate θ it was assumed that the oil, water and ash were actually medicinal glycerol. The resulting error in θ of ~ 15% is inconsequential. Fig. 7 shows that there was more CO and less CO_2, when the fuel was waste glycerol, rather than the pure medicinal variety [8]. This observation is confirmed below in Fig. 8. Also, the axial profiles in Fig. 7 are interesting, with minima for CO and CO_2. Part of the explanation is that the organic waste oils in industrial glycerol, being somewhat heavier and less volatile than glycerol, pass right through the bed inside bubbles of fuel and leave the bed un-oxidised after being only slightly heated and pyrolysed. Immediately above the fluidised particles, in the near-turbulent splash-zone, bubbles burst and their contents mix with the surrounding gas. Even so, bubbles can often retain their identity [37] for the first ≈ 300 mm of the freeboard. In addition, the centre-line of the freeboard is fuel-rich, but the gas near the containing wall above the bed is oxygen-rich. This requires oxygen to diffuse inwards towards the centre-line, whilst carbonaceous species diffuse radially outwards. One consequence is that with industrial glycerol in Fig. 7, after bubbles have disengaged from the sand and their contents have mixed somewhat, there is secondary combustion (particularly of hydrocarbons from the oily, less combustible, non-glycerides). This produces more CO and CO_2, starting at ~ 300 mm above the bed, according to Fig. 7. It is notable that beyond ~ 300 mm above the bed, CO was detected when burning the industrial fuel, but not for medicinal glycerol. Another part of this picture is that vapours of waste glycerol, contain the less volatile waste oils, which pyrolyse more slowly than glycerol, when passing through a bed, without being totally oxidised to CO or CO_2. Of course, combustion within a fluidised bed is limited by the contents of largish bubbles of gas being slow to mix with that gas passing interstitially between the fluidised particles of SiO_2 [26,34,38]. A final complicating feature of sampling the off-gases from a fluidised bed is that atmospheric air can enter a sample taken from the very top of the tube housing the bed [39]. However, the profiles in Fig. 7 demonstrate that this did not occur to increase the concentration of O_2 or diminish the concentration profiles of CO or CO_2.

Fig. 7 is related to the easily audible "popping" noises and to the sooting yellow flames, seen to extend 20 to 30 cm above the bed. The sooty flames were more intense when burning waste, rather than medicinal glycerol, especially in more fuel-rich situations (for comparison see FigS. 1 and 2 in the Supplementary Document). To form soot these yellow flames require a hydrocarbon to be present in the fuel, so their fragments must derive from organic, non-glycerides passing unreacted through a bed inside bubbles of industrial glycerol. The "popping" sounds were not as brief or as loud as those from burning medicinal glycerol, when these noises were attributed [8] to hydrogen (from the pyrolysis of medicinal glycerol) burning. Now, when burning waste glycerol, the emitted sounds were similar to those heard when fluidising a hot bed of sand with a mixture of methane and air, or propane and air [34,40]. It seems that when burning waste glycerol, the actual glycerol component does decompose thermally in ascending bubbles to yield CO and H_2, together with some other hydrocarbons and soot. The hydrocarbons and CO burn above the bed emitting sooting flames, blue flashes and loud popping sounds.

3.5. Varying the equivalence Ratio, θ

The combustion of medicinal glycerol has been shown to be largely insensitive to temperature, but strongly affected by θ [8]. In addition, CO was not then significantly produced when θ less than 0.7; also, it was found that for $\theta > 0.7$ the mole fraction of CO_2 was roughly constant at

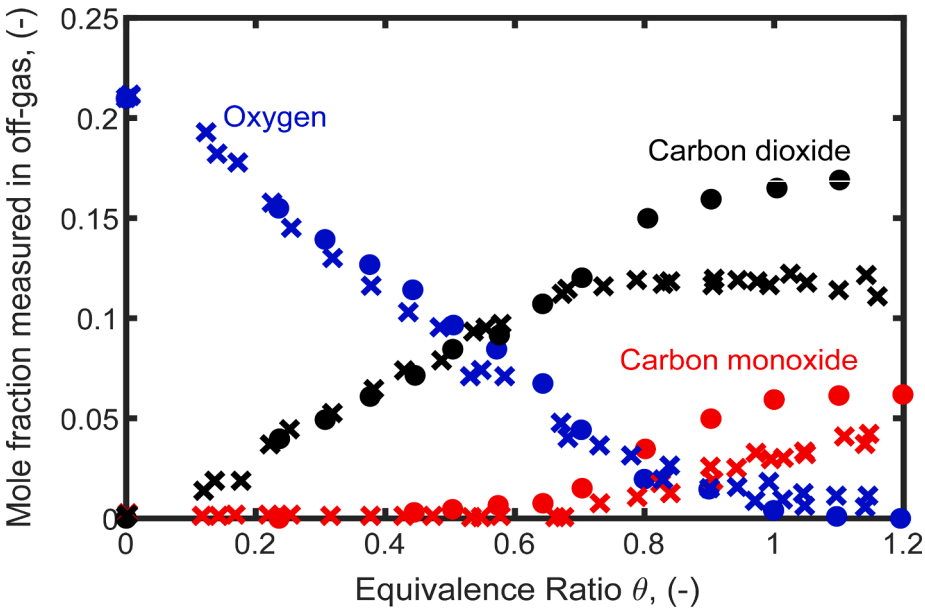

Fig. 8. Mole fractions of CO, CO_2 and O_2, measured at different equivalence ratios, θ, for industrial glycerol (●) with the bed at 750 °C, and (×) for medicinal glycerol with the bed at 700 °C taken from Gibson *et al.* [8]. Sampling was on the axis, 33 cm above the top of the fluidised bed; the values plotted were averages of measurements taken over 10 min. Their errors are ±0.005.

0.12. Fig. 8 presents measurements from burning waste or medicinal glycerol in a bed of SiO_2 particles, when varying θ. For these experiments, the flowrate of air was kept constant, but that of the glycerol under study was varied. By increasing θ in Fig. 8 by a factor of ~ 12, according to Eq. (1) the volume of a fuel bubble grew by a factor of $12^{6/5}$. This means that the initial diameter of a bubble of fuel increased $12^{2/5}$, *i.e.* 2.7 times, in changing θ from 0.1 to 1.2. In addition, the rise-velocity, U_b, of a bubble varies as $d^{1/2}$, according to Eq. (2), so that in changing from fuel-lean to fuel-rich, U_b increased by a factor of 1.64.

Fig. 8 shows that small amounts of CO appeared when burning waste glycerol with $\theta > 0.5$, *i.e.*, significantly lower than the threshold at $\theta = 0.7$ for medicinal glycerol. This might be explained by slightly smaller concentrations of O_2, as Fig. 8 shows. More CO was found by burning waste glycerol than medicinal glycerol. Oxygen appears to be totally consumed at $\theta > 1$ with the industrial fuel. The mole fraction of CO_2 plateaus for $\theta > \sim 0.7$ with industrial glycerol, when it reaches 0.17, *i.e.* higher than the maximum level (0.12) for medicinal glycerol. This indicates a high conversion to CO_2 and agrees with the fact that the fuel contained waste, fairly heavy oils. It aligns with the observation that combustion was self-sustained, so that no external heating was required, and indeed the external heaters automatically switched off and yet the bed's temperature was maintained at 750 °C. This amounts to the successful combustion of waste glycerol, reported here for the first time in a fluidised bed.

Further work will fluidise alternative solids, as well as vary the depth of the sand, the size of the particles and U/U_{mf}. The way of injecting waste glycerol into the bottom bed will be improved to reduce the initial size of bubbles of both air and waste glycerol entering the bed.

4. Conclusions

Burning industrial glycerol in a fluidised bed is more challenging than burning medicinal glycerol. Even so, much has been learned about the many processes occurring. Silica sand is so far the best material to be used in a fluidised bed for burning waste glycerol. With it, combustion lasted for a total of ~ 4 h, before the onset of sintering. The profiles of gas concentrations above the bed indicated more CO_2 and CO than in the combustion of medicinal glycerol. This must be attributed to the organic, non-glycerides present in waste glycerol. These oils are heavier and less volatile than glycerol. When the equivalence ratio, θ, was varied, it was found that CO appeared at a lower θ than when burning medicinal glycerol, possibly because it was not being so readily oxidised to CO_2. Also, the silica sand changed colour from yellow to grey, and once the colour change was complete, the particles sintered, i.e., the silica particles agglomerated and limited the usable life of the sand. Slightly sooting flames were usually observed above the bed, suggesting that, at these temperatures and with beds ~ 25 cm deep, vapour from waste glycerol was not fully mixing inside a bed with the O_2 in the fluidising air.

Clearly, there is more work to be done on the enigmatic agglomeration of the fluidised particles. This study was novel in that the fuel was a liquid, in contrast to *e.g.* solid biomass or coal. Here it seems that the fuel enters the hot bed as bubbles of waste glycerol. These burn individually and leave a tiny molten droplet, or maybe a solid particle, of *e.g.* potassium sulphate, together with possibly its hydroxide. Then it looks as if such a melt actually wets or binds to alumina particles more tightly than ones of silica. After much research [22,28], understanding of how sinters are formed is still sketchy at best.

Declaration of Competing Interest

The authors declare that they have no known competing financial interests or personal relationships that could have appeared to influence the work reported in this paper.

Acknowledgements

The authors warmly thank Dr Jason Day for his help in performing the ICP-MS analysis, and Mr Alexander Harrison for help with the XRD and SEM-EDS analysis. They are also grateful to David Jackson of Argent Energy, Motherwell, Scotland for generously providing samples of waste, industrial glycerol, as well as useful discussions.

Appendix A. Supplementary data

Supplementary data to this article can be found online at https://doi.org/10.1016/j.fuel.2022.124169.

References

[1] Weinberg FJ. Advanced combustion methods. Academic Press; 1986.
[2] Quispe CAG, Coronado CJR, Carvalho Jr JA. Glycerol: Production, consumption, prices, characterization and new trends in combustion. Renew Sustain Energy Rev 2013;27:475–93.
[3] Fangrui M, Milford HA. Biodiesel production: a review. Bioresour Technol 1999; 70:1–15.
[4] André Cremonez P, Feroldi M, Cézar Nadaleti W, de Rossi E, Feiden A, de Camargo MP, et al. Biodiesel production in Brazil: Current scenario and perspectives. Renew Sustain Energy Rev 2015;42:415–28.
[5] Monteiro MR, Kugelmeier CL, Pinheiro RS, Batalha MO, A. da Silva César, Glycerol from biodiesel production: Technological paths for sustainability. Renew Sustain Energy Rev 2018;88:109–22.
[6] Siles López José Ángel, Martín Santos María de los Ángeles, Chica Pérez Arturo Francisco, Martín Martín Antonio. Martín Martín, Anaerobic digestion of glycerol derived from biodiesel manufacturing. Bioresour Technol 2009;100(23):5609–15.
[7] Grammelis P. Solid Biofuels for Energy: A Lower Greenhouse Gas Alternative. London: Springer-Verlag; 2011.
[8] Gibson Ian, Slim Chris J, Zheng Yaoyao, Scott Stuart A, Davidson John F, Hayhurst Allan N. The continuous combustion of glycerol in a fluidised bed. Combust Flame 2019;200:60–8.
[9] Hayhurst AN, Tucker RF. The combustion of carbon monoxide in a two-zone fluidized bed. Combust Flame 1990;79(2):175–89.
[10] Bohon Myles D, Metzger Brian A, Linak William P, King Charly J, Roberts William L. Glycerol combustion and emissions. Proc Combust Inst 2011;33(2):2717–24.
[11] Menon A, Waller N, Hu W, Hayhurst AN, Davidson JF, Scott SA. The combustion of solid paraffin wax and of liquid glycerol in a fluidised bed. Fuel 2017;199:447–55.
[12] Stubington JF, Davidson JF. Gas-phase combustion in fluidized beds. AIChE J 1981;27:59–65.
[13] M. Miccio, F. Miccio, Fluidized Combustion of Liquid Fuels: Pioneering Works, Past Applications, Today's Knowledge and Opportunities, in: G. Yue, H. Zhang, C. Zhao, Z. Luo (Eds.), Proc. 20th Int. Conf. Fluid. Bed Combust., Springer, Berlin, Heidelberg, 2010: pp. 71–82.
[14] Okasha FM, El-Emam SH, Mostafa HK. The fluidized bed combustion of a heavy liquid fuel. Exp Therm Fluid Sci 2003;27:473–80.
[15] Steinmetz SA, Herrington JS, Winterrowd CK, Roberts WL, Wendt JOL, Linak WP. Crude glycerol combustion: Particulate, acrolein, and other volatile organic emissions. Proc Combust Inst 2013;34:2749–57.
[16] Arntz D, Fischer A, Höpp M, Jacobi S, Sauer J, Ohara T, et al. Ullmanns Encycl Ind Chem, American Cancer Society 2007.
[17] Żukowski W, Berkowitz G. The combustion of liquids and low-density solids in a cenospheric fluidised bed. Combust Flame 2019;206:476–89.
[18] Basu P, Sarka A. Agglomeration of coal ash in fluidized beds. Fuel 1983;62:924–6.
[19] Datta S, Sarkar P, Chavan PD, Saha S, Sahu G, Sinha AK, et al. Agglomeration behaviour of high ash Indian coals in fluidized bed gasification pilot plant. Appl Therm Eng 2015;86:222–8.
[20] Ergudenler A, Ghaly AE. Quality of gas produced from wheat straw in a dual-distributor type fluidized bed gasifier. Biomass Bioenergy 1992;3:419–30.
[21] Ghaly AE, Ergüdenler A, Laufer E. Agglomeration characteristics of alumina sand - straw ash mixtures at elevated temperatures. Biomass Bioenergy 1993;5:467–80.
[22] Morris JD, Daood SS, Chilton S, Nimmo W. Mechanisms and mitigation of agglomeration during fluidized bed combustion of biomass: A review. Fuel 2018; 230:452–73.
[23] T. McCann, Can Industrial Waste Glycerol be Burned in a Fluidised Bed?, M.Eng. Thesis, University of Cambridge, Department of Chemical Engineering and Biotechnology, 2019.
[24] Davidson JF, Harrison D. Fluidised particles. Cambridge: University Press; 1963.
[25] Kunii D, Levenspiel O. Fluidisation Engineering. Malabar, Florida: Krieger; 1969.
[26] Dennis JS, Hayhurst AN, Mackley IG. The ignition and combustion of propane/air mixtures in a fluidised bed. Proc Combust Inst 1982;19:1205–12.
[27] Chirone R, Miccio F, Scala F. Mechanism and prediction of bed agglomeration during fluidized bed combustion of a biomass fuel; effect of reactor scale. Chem Eng J 2006;123:71–80.
[28] Scala F. Particle agglomeration during fluidized bed combustion: Mechanisms, early detection and possible countermeasures. Fuel Proc Technol 2018;171:31–8.
[29] K. Schofield, The flame chemistry of alkali and alkaline earth metals, in: A. Fontijn (Ed.), Gas Phase Met. React., Elsevier, Amsterdam, 1992: pp. 529–571.
[30] Olofsson G, Ye Z, Bjerle I, Andersson A. Bed Agglomeration Problems in Fluidized-Bed Biomass Combustion. Ind Eng Chem Res 2002;41:2888–94.
[31] Sevonius C, Yrjas P, Hupa M. Defluidization of a quartz bed - laboratory experiments with potassium salts. Fuel 2014;127:161–8.
[32] Ma T, Fan C, Hao L, Li S, Song W, Lin W. Biomass - ash induced agglomeration in a fluidized bed, Part 1: Experimental study on the effects of a gas atmosphere. Energy Fuel 2016;30:6395–404.
[33] Zihms SG, Switzer C, Irvine J, Karstunen M. Effects of high temperature processes on physical properties of silica sand. Eng Geol 2013;164:139–45.
[34] Chadeesingh DR, Hayhurst AN. The combustion of a fuel-rich mixture of methane and air in a bubbling fluidised bed of silica sand at 700°C and also with particles of Fe_2O_3 or Fe present. Fuel 2014;127:169–77.
[35] Hayhurst AN. The ignition and combustion of mixtures of a gaseous hydrocarbon fuel when fluidising a bed of sand. Combust Flame 2022;240:112044.
[36] Jensen DE, Jones GA. Reaction rate coefficients for flame calculations. Combust Flame 1978;32:1–34.
[37] Müller CR, Hartung G, Hult J, Dennis JS, Kaminski CF. Laser diagnostic investigation of the bubble eruption patterns in the freeboard of fluidized beds: Simultaneous acetone PLIF and stereoscopic PIV measurements. AIChE J 2009;55: 1369–82.
[38] Pilawska M, Butler CJ, Hayhurst AN, Chadeesingh DR. The production of nitric oxide during the combustion of methane and air in a fluidised bed. Combust Flame 2001;127:2181–93.
[39] Fennell PS, Dennis JS, Hayhurst AN. The order with respect to oxygen and the activation energy for the burning of an anthracitic char in O_2 in a fluidised bed, as measured using a rapid analyser for CO and CO_2. Proc Combust Inst 2009;32: 2051–8.
[40] Hayhurst AN, John JJ, Wazacz RJ. The combustion of propane and air as catalyzed by platinum in a fluidised bed of hot sand. Proc Combust Inst 1998;27:3111–8.